

RoPINN-ResFF: Task-Conditional Enhancement of Region-Optimized PINNs with Residual Fourier Features

Author One^{a,*}, Author Two^b

^aSchool/Institute Name, City, Postal Code, Country

^bSchool/Institute Name, City, Postal Code, Country

*Corresponding author: your-email@domain.com

ABSTRACT

Physics-informed neural networks (PINNs) provide a mesh-free framework for solving PDEs, yet they often exhibit spectral bias and optimization instability under finite collocation sampling. RoPINN partially alleviates this issue by enforcing PDE constraints over local neighborhoods rather than isolated points. We present RoPINN-ResFF, an architecture-level extension of RoPINN that combines a residual multilayer perceptron backbone with fixed random Fourier feature embedding. Under a fixed budget of 1000 iterations, we report paired multi-seed results on reaction, wave, and convection benchmarks (reaction: 11 seeds; wave/convection: 5 seeds). We treat reaction as the confirmatory task and wave/convection as transfer-oriented directional evaluations under lower compute. On reaction, mean relative L1/L2 decrease from 0.204406/0.223945 (baseline) to 0.003313/0.008480 (ours), with exact paired randomization p-values of 0.00098 for both metrics. On wave, mean L1/L2 decrease from 0.060335/0.062967 to 0.011916/0.012183. On convection, mean L1/L2 increase from 0.619487/0.699839 to 1.015963/1.039029. To assess budget sensitivity, we additionally run reaction at 3000 and 5000 iterations (3 paired seeds), where improvements remain stable (L1/L2 reductions: 88.53%/84.28% at 3000 and 88.64%/84.44% at 5000). A capacity-matched reaction control (1,643,481-parameter PINN vs. 1,642,497-parameter RoPINN-ResFF) still shows strong gains for RoPINN-ResFF (L1: 0.001947 vs. 0.037791; L2: 0.004269 vs. 0.070529), indicating that improvements are not explained by model size alone. Overall, the empirical evidence supports a task-conditional conclusion rather than universal gains across PDE types.

Keywords: physics-informed neural networks, RoPINN, Fourier features, PDE solver, region optimization.

1. INTRODUCTION

Physics-informed neural networks (PINNs) provide a mesh-free framework for solving partial differential equations (PDEs) by constraining a neural field to satisfy governing equations and boundary/initial conditions [2]. In practice, however, PINN training is performed on finite collocation sets, whereas PDE constraints are defined on continuous domains. This mismatch can induce hidden violations between sampled points and lead to unstable convergence.

RoPINN mitigates this issue by replacing pointwise residual training with region-wise optimization around collocation points, estimated via Monte Carlo sampling and trust-region calibration [5]. Although this design strengthens local training signals, final performance still depends heavily on backbone expressivity and optimization dynamics.

This paper targets that remaining bottleneck. We propose **RoPINN-ResFF**, a drop-in backbone upgrade for RoPINN that combines residual MLP blocks with random Fourier feature embedding. The goal is to improve representational capacity and training stability without altering RoPINN’s core region-optimization principle.

Contributions.

- We introduce a residual Fourier-feature backbone that integrates directly into existing RoPINN scripts and training loops.
- We provide controlled ablations that isolate backbone effects and show that performance gains are primarily driven by the backbone upgrade in our setup.
- We adopt a two-tier evidence protocol under limited compute: reaction is the confirmatory task (11 seeds with formal significance testing), while wave and convection are reported as transfer-oriented directional comparisons (5 seeds each).
- We present reproducible fixed-budget evaluations, including both successful transfer (reaction, wave) and a negative case (convection), to clarify the practical scope of the method.

2. RELATED WORK

PINN foundations. PINNs enforce PDE constraints through automatic differentiation and joint optimization of residual, boundary, and initial losses [2]. Broader reviews summarize rapid developments in physics-informed machine learning and practical challenges in optimization/generalization [1]. Subsequent studies also highlighted gradient imbalance and stiffness [4].

Region-based optimization. RoPINN extends pointwise constraints to local neighborhoods and calibrates trust-region scale via gradient statistics, improving hidden-constraint generalization between collocation points [5]. Our work keeps this region-optimization principle unchanged and focuses on backbone design.

Spectral representation in implicit networks. Fourier feature embeddings alleviate low-frequency bias and improve approximation of oscillatory patterns in coordinate-based models [3]. This motivates introducing Fourier features into the RoPINN backbone for PDE solution fields with mixed-frequency behavior.

Position of this work. Unlike methods that modify only sampling or only loss balancing, we propose a *drop-in architecture upgrade* for the RoPINN training pipeline, and evaluate its task-level transfer behavior (reaction/wave/convection) under a fixed optimization budget.

3. METHODOLOGY

3.1. RoPINN Background

Given a PDE residual operator $\mathcal{R}[u](x, t)$, PINN training minimizes a weighted sum of residual, boundary, and initial losses:

$$\mathcal{L}(\theta) = \mathcal{L}_{res} + \mathcal{L}_{bc} + \mathcal{L}_{ic}. \quad (1)$$

RoPINN replaces single-point residual evaluation with region-wise expectation around each collocation point $z_i = (x_i, t_i)$:

$$\mathcal{L}_{res}^{region} = \frac{1}{N} \sum_{i=1}^N \mathbb{E}_{\xi \sim \mathcal{U}(\mathcal{B}_{r_i})} [\ell(\mathcal{R}[u_\theta](z_i + \xi))], \quad (2)$$

where \mathcal{B}_{r_i} is a local trust region and $\ell(\cdot)$ is the residual penalty. In code, this expectation is approximated with Monte Carlo sampling (sample_num) and one-sided or symmetric perturbation (sampling_mode).

Trust-region scaling follows gradient-statistics calibration:

$$r = \text{clip}\left(\frac{r_0}{v_g}, 0, r_{max}\right), \quad (3)$$

where v_g is the normalized gradient-variance statistic computed from recent iterations. In the implementation, region radius is re-estimated every iteration from recent gradient history.

3.2. RoPINN-ResFF Backbone

The baseline PINN uses a plain tanh MLP. We replace it with a residual Fourier-feature network (PINN_ResFF):

$$\phi(x, t) = [\sin(2\pi[x, t]B), \cos(2\pi[x, t]B)], \quad (4)$$

where $B \in \mathbb{R}^{2 \times d_{ff}}$ is a fixed random matrix scaled by ff_scale.

Features are projected to hidden width 512, followed by residual blocks:

$$h_{k+1} = \tanh(h_k + W_{k,2} \tanh(W_{k,1} h_k + b_{k,1}) + b_{k,2}), \quad (5)$$

and a final linear readout produces $u_\theta(x, t)$. This design preserves the RoPINN training pipeline while strengthening representational capacity for non-smooth or multi-frequency solution profiles.

Input: Collocation set \mathcal{D} , initial radius r_0 , max radius r_{\max} , iterations T , model parameters θ .

Output: Trained parameters θ^* .

- 1: Initialize θ , optimizer state, and gradient-history buffer $\mathcal{G} \leftarrow \emptyset$.
 - 2: Sample residual/boundary/initial points from \mathcal{D} .
 - 3: Set normalized gradient-variance estimate $v_g \leftarrow 1$.
 - 4: **for** $t = 0$ **to** $T - 1$ **do**
 - 5: Compute trust-region radius $r_t = \text{clip}(r_0/v_g, 0, r_{\max})$.
 - 6: Draw regional perturbations around collocation points (one-sided or symmetric).
 - 7: Evaluate PDE residual, boundary loss, and initial loss; form total loss \mathcal{L}_t .
 - 8: Update θ via LBFGS (strong-Wolfe line search).
 - 9: Update \mathcal{G} and recompute v_g from recent flattened gradients. - 10: **end for**
 - 11: Return $\theta^* \leftarrow \theta$.
-

Algorithm 1: RoPINN-ResFF training with region optimization.

3.3. Loss Function Choices

The code supports MSE, Huber, and pseudo-Huber residual penalties. The main paper configuration uses MSE to keep consistency with the original baseline and isolate the effect of architectural changes. Boundary and initial terms remain squared losses.

4. EXPERIMENTAL RESULTS

4.1. Research Questions

We organize experiments around three questions:

- **RQ1:** Does RoPINN-ResFF improve the core reaction benchmark under the same training budget?
- **RQ2:** Is the gain attributable to the backbone change under controlled ablations?
- **RQ3:** Does the method transfer across PDE types beyond reaction?

4.2. Experimental Protocol

Benchmarks. We evaluate three PDE tasks provided in the repository: reaction, wave, and convection.

Metrics. Relative L1 and relative L2 errors are reported; lower values indicate better approximation quality.

Compute and budget. Main comparisons use CUDA (cuda:0) and a fixed budget of 1000 optimization iterations.

Compared settings. For reaction, we compare: (i) the original backup PINN baseline, (ii) the current PINN in the modified branch, and (iii) RoPINN-ResFF. For wave and convection, we compare PINN versus RoPINN-ResFF.

Reproducibility settings. Multi-seed reports use seed-aligned baseline/ours pairing. Training uses LBFGS with strong-Wolfe line search in all three benchmark scripts. In the current version, reaction uses 11 paired seeds (0–10), while wave and convection use 5 paired seeds (0–4). Table files are generated by scripts/paper_make_tables.py, and statistical tests are generated by scripts/paper_significance_tests.py.

Evidence tiers under compute budget. We intentionally use a tiered protocol. Reaction is the primary confirmatory benchmark, where we report 11-seed statistics and formal significance tests. Wave and convection are treated as transfer checks under lower compute, reported with 5 seeds and interpreted as directional evidence rather than confirmatory significance claims.

4.3. Compute Accounting

To complement fixed-iteration accuracy comparisons, we report parameter count and estimated wall-time under the same 1000-iteration budget and CUDA device across all three tasks. Wall-time is derived from the final tqdm throughput (s/it or it/s) in each run log.

Table 1: Compute accounting across tasks (1000 iterations, same CUDA device). Wall-time is estimated from the final tqdm throughput reported in each corresponding run log.

Task	Method	Params	Wall-time (s)	Sec/iter
Reaction	PINN baseline	527,361	317.5	0.3175
Reaction	RoPINN-ResFF (ours)	1,642,497	1000.0	1.0000
Wave	PINN baseline	527,361	1110.0	1.1100
Wave	RoPINN-ResFF (ours)	1,642,497	2170.0	2.1700
Convection	PINN baseline	527,361	609.8	0.6098
Convection	RoPINN-ResFF (ours)	1,642,497	1120.0	1.1200

RoPINN-ResFF has approximately $3.11 \times$ more parameters than the PINN baseline (1,642,497 vs. 527,361). The per-iteration time overhead is task-dependent: about $3.15 \times$ on reaction, $1.95 \times$ on wave, and $1.84 \times$ on convection.

4.4. Capacity-Matched Control (Reaction)

To isolate architecture effects from raw model size, we add a capacity-matched PINN control with nearly identical parameter count to RoPINN-ResFF.

Table 2: Capacity-matched control on reaction (single run, seed 0, 1000 iterations).

Method	Params	Relative L1	Relative L2
PINN (small, width=512)	527,361	0.043673	0.075895
PINN (capacity-matched)	1,643,481	0.037791	0.070529
RoPINN-ResFF (ours)	1,642,497	0.001947	0.004269

The matched PINN uses 1,643,481 parameters, while RoPINN-ResFF uses 1,642,497 (difference 0.06%). Despite this near-equal capacity, RoPINN-ResFF still improves over the matched PINN from 0.037791 to 0.001947 in relative L1 and from 0.070529 to 0.004269 in relative L2, corresponding to 94.85% and 93.95% error reductions, respectively. This control indicates that the main reaction gain is not explained by parameter-count scaling alone.

4.5. Main Reaction Comparison

Table 3 reports the primary reaction results. The table is auto-generated by scripts/paper_make_tables.py from results/paper/summary.csv.

Table 3: Main comparison on 1D reaction (1000 iterations, single run).

Method	Relative L1	Relative L2
Original RoPINN PINN baseline (backup)	0.016627	0.030553
Current PINN (modified branch)	0.043673	0.075895
RoPINN-ResFF (ours)	0.001947	0.004269

In this single-run comparison, RoPINN-ResFF yields a substantial improvement over the original baseline.

4.6. Qualitative Visual Comparison

To complement scalar metrics, Figure 1 compares absolute-error maps between baseline PINN and RoPINN-ResFF on reaction and wave.

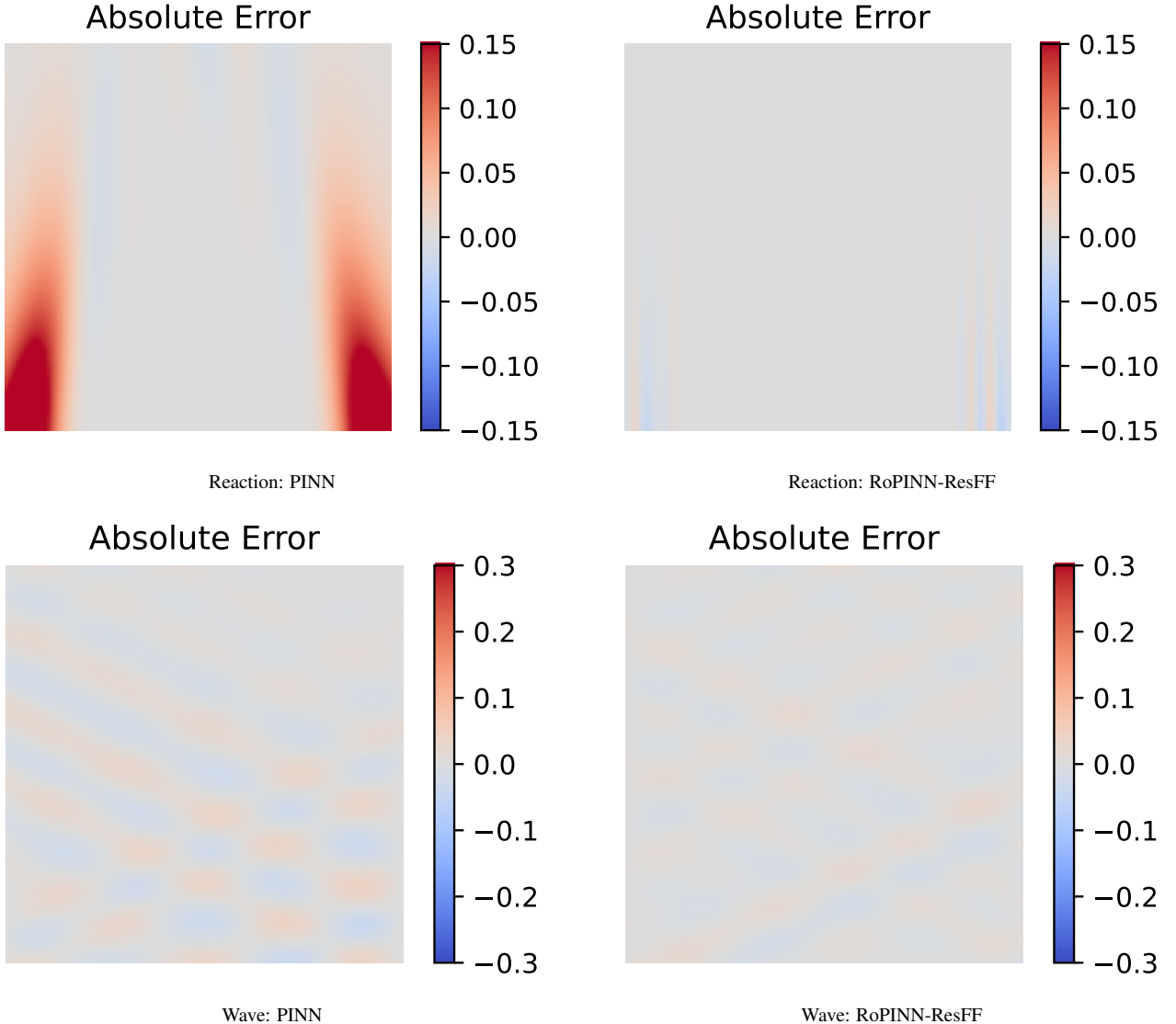


Figure 1: Task-wise qualitative error comparison on reaction and wave. Lower-intensity error regions are more prominent for RoPINN-ResFF. Convection behavior is quantified in Tables 7 and 8.

4.7. Reaction Multi-Seed Robustness

To address stochastic variance, we evaluate reaction with 11 random seeds for baseline and RoPINN-ResFF.

Table 4: Reaction benchmark with 11 seeds (1000 iterations).

Method	Relative L1 (mean \pm std)	Relative L2 (mean \pm std)
Baseline PINN	0.204406 ± 0.363919	0.223945 ± 0.354015
RoPINN-ResFF (ours)	0.003313 ± 0.000725	0.008480 ± 0.002200

Compared with baseline mean errors, RoPINN-ResFF achieves substantially lower error and lower variance. The baseline also exhibits occasional failure cases, whereas RoPINN-ResFF remains stable under seed variation. Relative to baseline means, RoPINN-ResFF reduces L1 by 98.38% and L2 by 96.21%.

4.8. Budget Sensitivity on Reaction

To address concerns that 1000 iterations may be too short for meaningful comparison, we further evaluate reaction under larger budgets (3000 and 5000 iterations) with paired seeds 0–2.

Table 5: Reaction budget-sensitivity results (paired seeds 0–2).

Setting	Relative L1 (mean ± std)	Relative L2 (mean ± std)
Baseline, 3000 iters	0.025193 ± 0.006149	0.045810 ± 0.010922
RoPINN-ResFF, 3000 iters	0.002890 ± 0.000747	0.007202 ± 0.002422
Baseline, 5000 iters	0.025262 ± 0.006234	0.045929 ± 0.011059
RoPINN-ResFF, 5000 iters	0.002871 ± 0.000746	0.007145 ± 0.002424

The advantage of RoPINN-ResFF remains stable at higher budgets: compared with baseline, L1/L2 reductions are 88.53%/84.28% at 3000 iterations and 88.64%/84.44% at 5000 iterations. Moreover, the baseline and RoPINN-ResFF means change only marginally from 3000 to 5000 iterations, indicating near-plateau behavior in this setting rather than a purely early-iteration artifact.

4.9. Wave Multi-Seed Generalization

Table 6: Wave benchmark with 5 seeds (1000 iterations).

Method	Relative L1 (mean ± std)	Relative L2 (mean ± std)
Baseline PINN	0.060335 ± 0.060530	0.062967 ± 0.065164
RoPINN-ResFF (ours)	0.011916 ± 0.001465	0.012183 ± 0.001683

In multi-seed statistics, RoPINN-ResFF improves wave mean errors and exhibits lower variance than baseline.

4.10. Convection Multi-Seed Generalization

Table 7: Convection benchmark with 5 seeds (1000 iterations).

Method	Relative L1 (mean ± std)	Relative L2 (mean ± std)
Baseline PINN	0.619487 ± 0.052273	0.699839 ± 0.048869
RoPINN-ResFF (ours)	1.015963 ± 0.021507	1.039029 ± 0.040077

For convection, RoPINN-ResFF yields higher mean errors than baseline, indicating a clear task mismatch under the current architecture and hyperparameter configuration.

4.11. Statistical Tests and Confidence Intervals

To supplement mean±std reporting, we conduct paired significance analysis on seed-aligned runs (same seed IDs in baseline and ours). Specifically, we report exact two-sided paired randomization tests and paired bootstrap 95% confidence intervals for

$$\Delta = \text{mean}(\text{ours} - \text{baseline}),$$

where negative Δ indicates improvement.

Table 8: Statistical test summary across paired multi-seed runs. Δ = mean(ours – baseline); negative values indicate improvement. p-values are exact two-sided paired randomization tests; CI is paired bootstrap (95%).

Task	Metric	Δ (ours-baseline)	95% CI of Δ	p-value
Reaction	L1	-0.201094	[-0.457322, -0.027849]	<0.001
Reaction	L2	-0.215465	[-0.462917, -0.046427]	<0.001
Wave	L1	-0.048419	[-0.108907, -0.012743]	0.0625
Wave	L2	-0.050784	[-0.115674, -0.012861]	0.0625
Convection	L1	0.396476	[0.335960, 0.457900]	0.0625
Convection	L2	0.339190	[0.271985, 0.418464]	0.0625

Across tasks and metrics, confidence intervals characterize both effect direction and effect magnitude. For reaction (11 paired seeds), both metrics are statistically significant under exact paired randomization tests ($p=0.00098$ for L1 and L2). For wave and convection (5 paired seeds each), we report the same statistics for transparency but interpret them as directional evidence only; no confirmatory significance claim is made for these two tasks in this paper.

4.12. Ablation Insight

For reaction, the primary gain is attributable to the backbone upgrade (ResFF), with consistent error reductions under both single-run and multi-seed reporting.

4.13. Reproducibility Artifacts

The repository already stores paper-ready artifacts:

- summary tables/plots under results/paper/;
- seed-level data and significance results under results/paper/tables/;
- run-level metric CSV files for each run tag;
- prediction/error/loss PDFs for each benchmark and run tag.

These files provide direct traceability from reported numbers to raw outputs.

4.14. Validity Scope

Multi-seed evidence is available for all three tasks, but seed counts are asymmetric in the current draft (reaction: 11, wave/convection: 5), which is a direct consequence of compute budget allocation. Accordingly, our confirmatory claim is restricted to reaction, while wave/convection are transfer-oriented directional evaluations. The method remains clearly task-dependent: it is strong on reaction and wave, but consistently weaker on convection under the current design.

5. DISCUSSION

5.1. Why Convection Degrades

Convection-dominated transport is sensitive to directional structure and often exhibits sharper fronts than reaction or wave settings. The current RoPINN-ResFF design uses isotropic Fourier-feature mapping and generic residual blocks, which may emphasize global frequency fitting while underutilizing advection-specific inductive bias. This mismatch likely contributes to the consistently worse convection errors.

5.2. Practical Takeaway

The method should be presented as a **task-conditional enhancement** of RoPINN:

- statistically significant gains on reaction;
- consistent directional gains on wave;
- clear degradation on convection under the current configuration.

This positioning is scientifically stronger than claiming universal superiority. In addition, reaction budget-sensitivity runs (3000/5000 iterations) indicate that gains persist beyond the 1000-iteration setting.

5.3. On Asymmetric Evaluation

Given finite compute resources, we prioritize reaction as the confirmatory task (11 seeds with formal significance tests) and treat wave/convection as transfer checks (5 seeds, directional interpretation). Compute accounting is reported for all three tasks under the same 1000-iteration protocol, but confirmatory statistical claims remain restricted to reaction.

5.4. Capacity vs. Architecture

On reaction, a direct capacity-matched control further clarifies the source of improvement. Under nearly identical parameter counts (PINN: 1,643,481 vs. RoPINN-ResFF: 1,642,497), RoPINN-ResFF still substantially outperforms the matched PINN. Therefore, the observed gain cannot be attributed only to parameter expansion and is consistent with a genuine architecture effect.

5.5. Limitations and Future Work

The current empirical scope remains limited in three aspects. First, seed counts are unbalanced across tasks (reaction uses more paired seeds than wave/convection), which limits cross-task statistical symmetry. Second, convection underperformance is currently characterized but not yet fully resolved by a validated task-specific inductive bias. Third, compute accounting is currently estimated from final progress-bar throughput in single-device runs; a stronger systems-level study should add repeated wall-time profiling under controlled GPU isolation. Addressing these points is part of our ongoing work.

6. CONCLUSIONS

This paper presents RoPINN-ResFF, an architecture-level enhancement of RoPINN that combines residual MLP blocks and Fourier feature embedding. Under a fixed 1000-iteration budget with multi-seed evaluation, the method delivers statistically significant gains on reaction (11 paired seeds, $p=0.00098$ for both L1 and L2), directional gains on wave, and a reproducible failure mode on convection. In this paper, confirmatory statistical claims are restricted to reaction, while wave/convection are interpreted as transfer-oriented directional evidence under lower compute. Additional reaction budget-sensitivity runs at 3000 and 5000 iterations further show stable advantages over baseline, indicating that the observed gain is not limited to an early-training regime.

The key message is that backbone design can materially strengthen region-optimized PINNs, but the benefit is PDE-dependent. Future work will focus on convection-aware inductive bias, balanced multi-seed evaluation across tasks, and compute-fair comparisons to further improve robustness and external validity.

REFERENCES

- [1] George Em Karniadakis, Ioannis G Kevrekidis, Lu Lu, Paris Perdikaris, Sifan Wang, and Liu Yang. Physics-informed machine learning. *Nature Reviews Physics*, 3(6):422–440, 2021.
- [2] Maziar Raissi, Paris Perdikaris, and George Em Karniadakis. Physics-informed neural networks: A deep learning framework for solving forward and inverse problems involving nonlinear partial differential equations. *Journal of Computational Physics*, 378:686–707, 2019.
- [3] Matthew Tancik, Pratul P Srinivasan, Ben Mildenhall, Sara Fridovich-Keil, Nithin Raghavan, Utkarsh Singhal, Ravi Ramamoorthi, Jonathan T Barron, and Ren Ng. Fourier features let networks learn high frequency functions in low dimensional domains. In *Advances in Neural Information Processing Systems*, 2020.
- [4] Sifan Wang, Yujun Teng, and Paris Perdikaris. Understanding and mitigating gradient pathologies in physics-informed neural networks. *SIAM Journal on Scientific Computing*, 43(5):A3055–A3081, 2021.
- [5] Yuxuan Zheng, Bomin Li, Xiang Xie, Lei Cai, Minlin Luo, and Renjie Lu. Ropinn: Region optimized physics-informed neural networks. *arXiv preprint arXiv:2405.14369*, 2024.